The Infinite Spherical Well

If we work in spherical coordinates with a potential that depends only on r (not on θ or ϕ), another new feature arises that will be important in our subsequent investigations of nuclear structure. When we search for separable solutions, of the form $\psi(r, \theta, \phi) = R(r)\,\Theta(\theta)\,\Phi(\phi)$, the central potential $V(r)$ appears only in the radial part of the separation equation, and the angular parts can be solved directly. The differential equation for $\Phi(\phi)$ is

$$\frac{d^2\Phi}{d\phi^2} + m_\ell^2\,\Phi = 0 \tag{2.57}$$

where m_ℓ^2 is the separation constant.

The solution is

$$\Phi_{m_\ell}(\phi) = \frac{1}{\sqrt{2\pi}}\,e^{im_\ell\phi} \tag{2.58}$$

where $m_\ell = 0, \pm 1, \pm 2, \ldots$. The equation for $\Theta(\theta)$ is

$$\frac{1}{\sin\theta}\frac{d}{d\theta}\left(\sin\theta\frac{d\Theta}{d\theta}\right) + \left[\ell(\ell+1) - \frac{m_\ell^2}{\sin^2\theta}\right]\Theta = 0 \tag{2.59}$$

where $\ell = 0, 1, 2, 3, \ldots$ and $m_\ell = 0, \pm 1, \pm 2, \ldots, \pm\ell$. The solution $\Theta_{\ell m_\ell}(\theta)$ can be expressed as a polynomial of degree ℓ in $\sin\theta$ or $\cos\theta$. Together, and normalized, $\Phi_{m_\ell}(\phi)$ and $\Theta_{\ell m_\ell}(\theta)$ give the *spherical harmonics* $Y_{\ell m_\ell}(\theta, \phi)$, some examples of which are listed in Table 2.2. These functions give the angular part of the solution to the Schrödinger equation for *any central potential* $V(r)$. For example, it is these angular functions that give the spatial properties of atomic orbitals that are responsible for molecular bonds.

For each potential $V(r)$, all we need to do is to find a solution of the radial equation

$$-\frac{\hbar^2}{2m}\left(\frac{d^2R}{dr^2} + \frac{2}{r}\frac{dR}{dr}\right) + \left[V(r) + \frac{\ell(\ell+1)\hbar^2}{2mr^2}\right]R = ER \tag{2.60}$$

Table 2.2 Spherical Harmonics for Some Low ℓ Values

ℓ	m_ℓ	$Y_{\ell m_\ell}(\theta, \phi) = \Theta_{\ell m_\ell}(\theta)\,\Phi_{m_\ell}(\phi)$
0	0	$(1/4\pi)^{1/2}$
1	0	$(3/4\pi)^{1/2}\cos\theta$
1	± 1	$\mp(3/8\pi)^{1/2}\sin\theta\,e^{\pm i\phi}$
2	0	$(5/16\pi)^{1/2}(3\cos^2\theta - 1)$
2	± 1	$\mp(15/8\pi)^{1/2}\sin\theta\cos\theta\,e^{\pm i\phi}$
2	± 2	$(15/32\pi)^{1/2}\sin^2\theta\,e^{\pm 2i\phi}$

$$\Phi_{m_\ell}(\phi) = \frac{1}{\sqrt{2\pi}}\,e^{im_\ell\phi}$$

$$\Theta_{\ell m_\ell}(\theta) = \left[\frac{2\ell+1}{2}\frac{(\ell-m_\ell)!}{(\ell+m_\ell)!}\right]^{1/2} P_\ell^{m_\ell}(\theta)$$

where $P_\ell^{m_\ell}(\theta)$ is the associated Legendre polynomial

77

Table 2.3 Spherical Bessel Functions — Sample Expressions and Limits

$$j_0(kr) = \frac{\sin kr}{kr}$$

$$j_1(kr) = \frac{\sin kr}{(kr)^2} - \frac{\cos kr}{kr}$$

$$j_2(kr) = \frac{3\sin kr}{(kr)^3} - \frac{3\cos kr}{(kr)^2} - \frac{\sin kr}{kr}$$

$$j_\ell(kr) \cong \frac{(kr)^\ell}{1 \cdot 3 \cdot 5 \cdots (2\ell+1)} \qquad kr \to 0$$

$$j_\ell(kr) \cong \frac{\sin(kr - \ell\pi/2)}{kr} \qquad kr \to \infty$$

$$j_\ell(kr) = \left(-\frac{r}{k}\right)^\ell \left(\frac{1}{r}\frac{d}{dr}\right)^\ell j_0(kr)$$

The $\ell(\ell+1)$ term is generally written as an addition to the potential; it is called the "centrifugal potential" and it acts like a potential that keeps the particle away from the origin when $\ell > 0$.

As an example, we consider the case of the infinite spherical well,

$$V(r) = 0 \qquad r < a$$
$$= \infty \qquad r > a \tag{2.61}$$

We require again that $R(r) = 0$ for $r > a$, since the walls of the infinite well are impenetrable. Inside the well, the solution to Equation 2.60 for $V = 0$ can be expressed in terms of the oscillatory functions known as *spherical Bessel functions* $j_\ell(kr)$, some of which are listed in Table 2.3. To find the energy eigenvalues, we proceed exactly as in the one-dimensional problem and apply the continuity condition on ψ at $r = a$. This gives

$$j_\ell(ka) = 0 \tag{2.62}$$

This is in effect a transcendental equation, which must be solved numerically. Tables of the spherical Bessel functions are available that can be consulted to find the zeros for any given value of ℓ.* For example, we consider the case $\ell = 0$. From the tables we find $j_0(x) = 0$ at $x = 3.14, 6.28, 9.42, 12.57$, and so on. For $\ell = 1$, the first few zeros of $j_1(x)$ are at $x = 4.49, 7.73, 10.90, 14.07$. Since $E = \hbar^2 k^2/2m$, we can then solve for the allowed values of the energies. Repeating this process for $\ell = 2$, $\ell = 3$, and so on, we would be able to construct a spectrum of the energy states, as is shown in Figure 2.11. As in the case of the Cartesian well, the regularity of the one-dimensional problem is not present. Also, note that the levels are again degenerate—since the energy depends only on ℓ, the wave functions with different m_ℓ values all have the same energy. Thus, in the case of the level with $\ell = 2$, the possible wave functions are $j_2(kr)Y_{22}(\theta, \phi)$,

* M. Abramowitz and I. A. Stegun, *Handbook of Mathematical Functions* (New York: Dover, 1965).

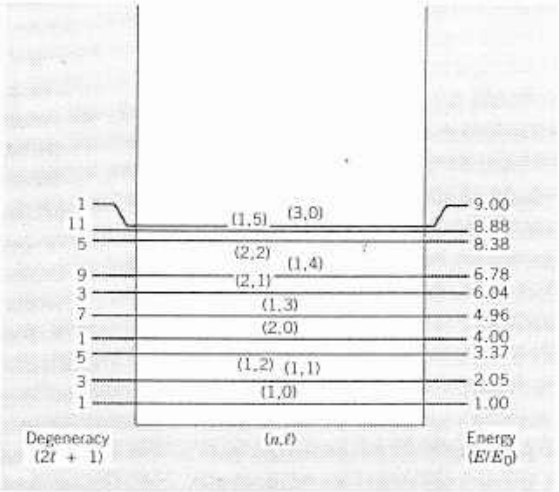

Figure 2.11 Energy levels of a particle confined to a three-dimensional spherical container. The energy is given in units of $E_0 = \hbar^2\pi^2/2ma^2$. Compare with the spacings and degeneracies of Figure 2.10. The quantum number n does not arise directly in the solution in this case; it serves to number the states of a given ℓ.

$j_2(kr)Y_{21}(\theta,\phi)$, $j_2(kr)Y_{20}(\theta,\phi)$, $j_2(kr)Y_{2-1}(\theta,\phi)$, and $j_2(kr)Y_{2-2}(\theta,\phi)$, for a fivefold degeneracy. In fact, since m_ℓ is restricted to the values 0, ± 1, $\pm 2, \ldots, \pm\ell$, there are exactly $2\ell+1$ possible $Y_{\ell m_\ell}$ for a given ℓ, and thus each level has a degeneracy of $2\ell+1$. (This situation is very similar to the case of electronic orbits in atoms, in which there is also a central potential. The capacity of each atomic subshell contains the factor of $2\ell+1$, which likewise arises from the m_ℓ degeneracy.)

The probability to locate the particle in a volume dv is given by $|\psi|^2\,dv$, where the volume element was given in Equation 2.17. Such three-dimensional distributions are difficult to represent graphically, so we often consider the radial and angular parts separately. To find the radial probability density, which gives the probability to find the particle between r and $r+dr$ averaged over all angles, we integrate the probability density over θ and ϕ:

$$P(r)\,dr = \int |\psi|^2\,dv$$

$$= r^2\,|R(r)|^2\,dr \int \sin\theta\,d\theta \int d\phi\,|Y_{\ell m_\ell}|^2 \qquad (2.63)$$

The spherical harmonics $Y_{\ell m_\ell}$ are themselves normalized, so that the integral gives 1, and thus

$$P(r) = r^2\,|R(r)|^2 \qquad (2.64)$$

Some sample radial probability distributions for the infinite well are shown in Figure 2.12.

The angular dependence of the probability density for any central potential is given by $|Y_{\ell m_\ell}(\theta,\phi)|^2$, some samples of which are illustrated in Figure 2.13.

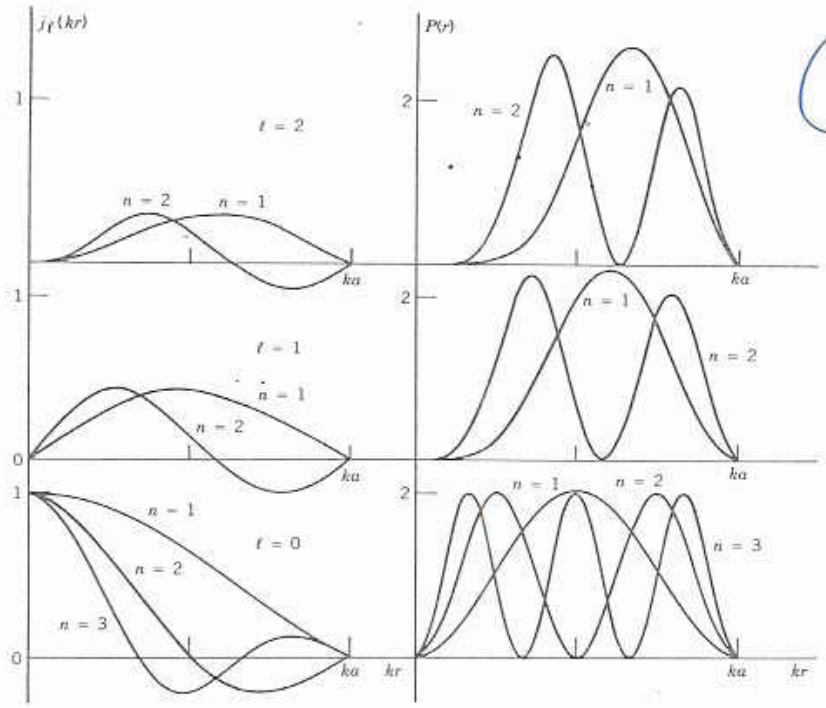

Figure 2.12 The left side shows, for some of the lower energy levels, the unnormalized $j_\ell(kr)$, adjusted so that $j_\ell(ka) = 0$. The right side shows the corresponding normalized radial probability density, r^2R^2. Note that all j_ℓ vanish at the origin except j_0, and that all probability densities vanish at $r = 0$. Also, note how the "centrifugal repulsion" pushes corresponding maxima in $P(r)$ away from the origin as ℓ increases.

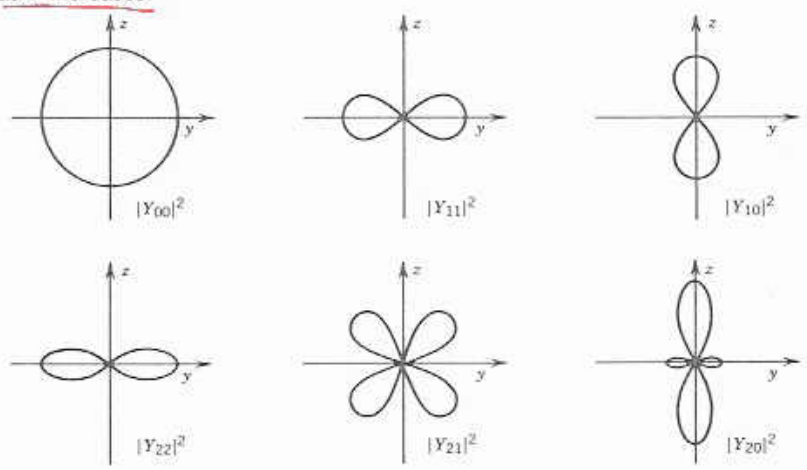

Figure 2.13 Spatial probability distributions resulting from the $Y_{\ell m_\ell}$. The three-dimensional representations can be obtained by rotating each figure about the z axis.

All of the previous considerations apply in this case as well, with the volume element

$$d\tau = r^2 \sin\theta \, dr \, d\theta \, d\phi \tag{2.17}$$

The following two sections illustrate the application of these principles, first with the mathematically simpler one-dimensional problems and then with the more physical three-dimensional problems.

2.3 PROBLEMS IN ONE DIMENSION

The Free Particle

For this case, no forces act and we take $V(x) = 0$ everywhere. We can then rewrite Equation 2.4 as

$$\frac{d^2\psi}{dx^2} = -\frac{2mE}{\hbar^2}\psi \tag{2.18}$$

The solution to this differential equation can be written

$$\psi(x) = A' \sin kx + B' \cos kx \tag{2.19}$$

or, equivalently

$$\psi(x) = A e^{ikx} + B e^{-ikx} \tag{2.20}$$

where $k^2 = 2mE/\hbar^2$ and where A and B (or A' and B') are constants.

The time-dependent wave function is

$$\Psi(x, t) = A e^{i(kx - \omega t)} + B e^{-i(kx + \omega t)} \tag{2.21}$$

The first term represents a wave traveling in the positive x direction, while the second term represents a wave traveling in the negative x direction. The intensities of these waves are given by the squares of the respective amplitudes, $|A|^2$ and $|B|^2$. Since there are no boundary conditions, there are no restrictions on the energy E; all values of E give solutions to the equation. The normalization condition 2.9 cannot be applied in this case, because integrals of $\sin^2$ or $\cos^2$ do not converge in $x = -\infty$ to $+\infty$. Instead, we use a different normalization system for such constant potentials. Suppose we have a source such as an accelerator located at $x = -\infty$, emitting particles at a rate I particles per second, with momentum $p = \hbar k$ in the positive x direction. Since the particles are traveling in the positive x direction, we can set B to zero—the intensity of the wave representing particles traveling in the negative x direction must vanish if there are no particles traveling in that direction. The particle current is, according to Equation 2.12,

$$j = \frac{\hbar k}{m}|A|^2 \tag{2.22}$$

which must be equal to the current of I particles per second emitted by the source. Thus we can take $A = \sqrt{mI/\hbar k}$.

(81)

Step Potential, $E > V_0$

The potential is

$$\begin{aligned} V(x) &= 0 \qquad x < 0 \\ &= V_0 \qquad x > 0 \end{aligned} \tag{2.23}$$

where $V_0 > 0$. Let us call $x < 0$ region 1 and $x > 0$ region 2. Then in region 1, the Schrödinger equation is identical with Equation 2.18 and the solutions ψ_1 are given by Equation 2.20 with $k = k_1 = \sqrt{2mE/\hbar^2}$. In region 2, the Schrödinger equation is

$$\frac{d^2\psi_2}{dx^2} = -\frac{2m(E - V_0)}{\hbar^2}\psi_2 \tag{2.24}$$

Since $E > V_0$, we can write the solution as

$$\psi_2 = Ce^{ik_2x} + De^{-ik_2x} \tag{2.25}$$

where $k_2 = \sqrt{2m(E - V_0)/\hbar^2}$.

Applying the boundary conditions at $x = 0$ gives

$$A + B = C + D \tag{2.26a}$$

from Equation 2.6*a*, and

$$k_1(A - B) = k_2(C - D) \tag{2.26b}$$

from Equation 2.6*b*.

Let's assume that particles are incident on the step from a source at $x = -\infty$. Then the A term in ψ_1 represents the *incident wave* (the wave in $x < 0$ traveling toward the step at $x = 0$), the B term in ψ_1 represents the *reflected wave* (the wave in $x < 0$ traveling back toward $x = -\infty$), and the C term in ψ_2 represents the *transmitted wave* (the wave in $x > 0$ traveling away from $x = 0$). The D term cannot represent any part of this problem because there is no way for a wave to be moving toward the origin in region 2, and so we eliminate this term by setting D to zero. Solving Equations 2.26*a* and 2.26*b*, we have

$$B = A\frac{1 - k_2/k_1}{1 + k_2/k_1} \tag{2.27}$$

$$C = A\frac{2}{1 + k_2/k_1} \tag{2.28}$$

The *reflection coefficient* R is defined as the current in the reflected wave divided by the incident current:

$$R = \frac{j_{\text{reflected}}}{j_{\text{incident}}} \tag{2.29}$$

and using Equation 2.22 we find

$$R = \frac{|B|^2}{|A|^2} = \left(\frac{1 - k_2/k_1}{1 + k_2/k_1}\right)^2 \tag{2.30}$$

The *transmission coefficient* T is similarly defined as the fraction of the incident

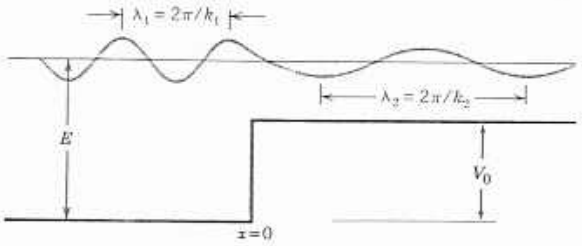

Figure 2.2 The wave function of a particle of energy E encountering a step of height V_0 for the case $E > V_0$. The de Broglie wavelength changes from λ_1 to λ_2 when the particle crosses the step, but ψ and $d\psi/dx$ are continuous at $x = 0$.

current that is transmitted past the boundary:

$$T = \frac{j_{\text{transmitted}}}{j_{\text{incident}}} \tag{2.31}$$

and thus

$$T = \frac{k_2}{k_1}\frac{|C|^2}{|A|^2} = \frac{4k_2/k_1}{(1 + k_2/k_1)^2} \tag{2.32}$$

Notice that $R + T = 1$, as expected. The resulting solution is illustrated in Figure 2.2.

This is a simple example of a *scattering* problem. In Chapter 4 we show how these concepts can be extended to three dimensions and applied to nucleon–nucleon scattering problems.

Step Potential, $E < V_0$

In this case, the potential is still given by Equation 2.23, and the solution for region 1 ($x < 0$) is identical with the previous calculation. In region 2, the Schrödinger equation gives

$$\frac{d^2\psi_2}{dx^2} = \frac{2m}{\hbar^2}(V_0 - E)\psi_2 \tag{2.33}$$

which has the solution

$$\psi_2 = Ce^{k_2 x} + De^{-k_2 x} \tag{2.34}$$

where $k_2 = \sqrt{2m(V_0 - E)/\hbar^2}$. Note that for *constant* potentials, the solutions are either oscillatory like Equation 2.19 or 2.20 when $E > V_0$, or exponential like Equation 2.34 when $E < V_0$. Although the mathematical forms may be different for nonconstant potentials $V(x)$, the general behavior is preserved: oscillatory (though not necessarily sinusoidal) when $E > V(x)$ and exponential when $E < V(x)$.

This solution, Equation 2.34, must be valid for the entire range $x > 0$. Since the first term would become infinite for $x \to \infty$, we must set $C = 0$ to keep the wave function finite. The D term in ψ_2 illustrates an important difference between classical and quantum physics, *the penetration of the wave function into*

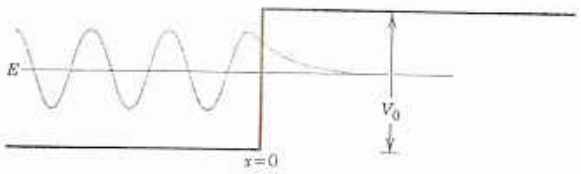

Figure 2.3 The wave function of a particle of energy E encountering a step of height V_0, for the case $E < V_0$. The wave function decreases exponentially in the classically forbidden region, where the classical kinetic energy would be negative. At $x = 0$, ψ and $d\psi/dx$ are continuous.

the classically forbidden region. All (classical) *particles* are reflected at the boundary; the quantum mechanical *wave packet*, on the other hand, can penetrate a short distance into the forbidden region. The (classical) particle is never directly *observed* in that region; since $E < V_0$, the kinetic energy would be negative in region 2. The solution is illustrated in Figure 2.3

Barrier Potential, $E > V_0$

The potential is

$$\begin{aligned} V(x) &= 0 \qquad x < 0 \\ &= V_0 \qquad 0 \le x \le a \\ &= 0 \qquad x > a \end{aligned} \tag{2.35}$$

In the three regions 1, 2, and 3, the solutions are

$$\begin{aligned} \psi_1 &= A e^{ik_1 x} + B e^{-ik_1 x} \\ \psi_2 &= C e^{ik_2 x} + D e^{-ik_2 x} \\ \psi_3 &= F e^{ik_3 x} + G e^{-ik_3 x} \end{aligned} \tag{2.36}$$

where $k_1 = k_3 = \sqrt{2mE/\hbar^2}$ and $k_2 = \sqrt{2m(E - V_0)/\hbar^2}$.

Using the continuity conditions at $x = 0$ and at $x = a$, and assuming again that particles are incident from $x = -\infty$ (so that G can be set to zero), after considerable algebraic manipulation we can find the transmission coefficient $T = |F|^2/|A|^2$:

$$T = \frac{1}{1 + \frac{1}{4}\frac{V_0^2}{E(E - V_0)}\sin^2 k_2 a} \tag{2.37}$$

The solution is illustrated in Figure 2.4.

Barrier Potential, $E < V_0$

For this case, the ψ_1 and ψ_3 solutions are as above, but ψ_2 becomes

$$\psi_2 = C e^{k_2 x} + D e^{-k_2 x} \tag{2.38}$$

where now $k_2 = \sqrt{2m(V_0 - E)/\hbar^2}$. Because region 2 extends only from $x = 0$

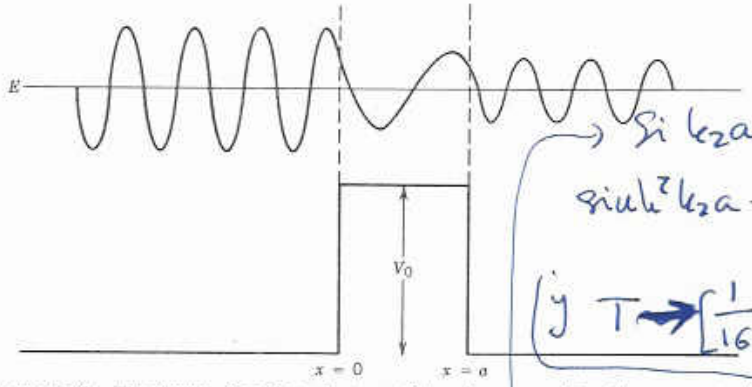

Figure 2.4 The wave function of a particle of energy $E > V_0$ encountering a barrier potential. The particle is incident from the left. The wave undergoes reflections at both boundaries, and the transmitted wave emerges with smaller amplitude.

to $x = a$, the question of an exponential solution going to infinity does not arise, so we cannot set C or D to zero.

Again, applying the boundary conditions at $x = 0$ and $x = a$ permits the solution for the transmission coefficient:

$$T = \frac{1}{1 + \frac{1}{4}\frac{V_0^2}{E(V_0 - E)}\sinh^2 k_2 a} \tag{2.39}$$

Classically, we would expect $T = 0$—the particle is not permitted to enter the forbidden region where it would have negative kinetic energy. The quantum wave can penetrate the barrier and give a nonzero probability to find the particle beyond the barrier. The solution is illustrated in Figure 2.5.

This phenomenon of *barrier penetration* or quantum mechanical *tunneling* has important applications in nuclear physics, especially in the theory of α decay, which we discuss in Chapter 8.

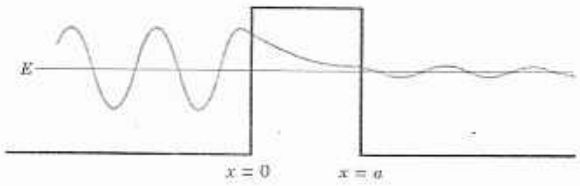

Figure 2.5 The wave function of a particle of energy $E < V_0$ encountering a barrier potential (the particle would be incident from the left in the figure). The wavelength is the same on both sides of the barrier, but the amplitude beyond the barrier is much less than the original amplitude. The particle can never be observed, inside the barrier (where it would have negative kinetic energy) but it can be observed *beyond* the barrier.

8 ALPHA DECAY

Alpha particles were first identified as the least penetrating of the radiations emitted by naturally occurring materials. In 1903, Rutherford measured their charge-to-mass ratio by deflecting α particles from the decay of radium in electric and magnetic fields. Despite the difficulty of these early experiments, Rutherford's result was only about 25% higher than the presently accepted value. In 1909 Rutherford showed that, as suspected, the α particles were in fact helium nuclei; in his experiments the particles entered an evacuated thin-walled chamber by penetrating its walls, and after several days of collecting, atomic spectroscopy revealed the presence of helium gas inside the chamber.

Many heavy nuclei, especially those of the naturally occurring radioactive series, decay though α emission. Only exceedingly rarely does any other spontaneous radioactive process result in the emission of nucleons; we do not, for example, observe deuteron emission as a natural decay process. There must therefore be a special reason that nuclei choose α emission over other possible decay modes. In this chapter we examine this question and study the α decay process in detail. We also show how α spectroscopy can help us to understand nuclear structure.

8.1 WHY α DECAY OCCURS

Alpha emission is a Coulomb repulsion effect. It becomes increasingly important for heavy nuclei because the disruptive Coulomb force increases with size at a faster rate (namely, as Z^2) than does the specific nuclear binding force, which increases approximately as A.

Why is the α particle chosen as the agent for the spontaneous carrying away of positive charge? When we call a process *spontaneous* we mean that some kinetic energy has suddenly appeared in the system for no apparent cause; this energy must come from a decrease in the mass of the system. The α particle, because it is a very stable and tightly bound structure, has a relatively small mass compared with the mass of its separate constituents. It is particularly favored as an emitted particle if we hope to have the disintegration products as light as possible and thus get the largest possible release of kinetic energy.

Ejercicio: (en grupos de hasta 5 como mucho) (86)

Reproducir la tabla 8.1 a partir de los datos de masas.

Table 8.1 Energy Release (Q value) for Various Modes of Decay of ^{232}U[a]

Emitted Particle	Energy Release (MeV)	Emitted Particle	Energy Release (MeV)
n	−7.26	^{4}He	+5.41
^{1}H	−6.12	^{5}He	−2.59
^{2}H	−10.70	^{6}He	−6.19
^{3}H	−10.24	^{6}Li	−3.79
^{3}He	−9.92	^{7}Li	−1.94
		^{12}C	?

[a]Computed from known masses.

For a typical α emitter ^{232}U (72 y) we can compute, from the known masses, the energy release for various emitted particles. Table 8.1 summarizes the results. Of the particles considered, spontaneous decay is energetically possible *only* for the α particle. A positive disintegration energy results for some slightly heavier particles than those listed, ^{8}Be or ^{12}C, for example. We will show, however (Section 8.4), that the partial disintegration constant for emission of such heavy particles is normally vanishingly small compared with that for α emission. Such decays would be so rare that in practice they would almost never be noticed. This suggests that if a nucleus is to be recognized as an alpha emitter it is not enough for α decay to be energetically possible. The disintegration constant must also not be too small or else α emission will occur so rarely that it may not be detected. With present techniques this means that the half-life must be less than about 10^{16} y. Also, β decay, if it has a much higher partial disintegration constant, can mask the α decay. Most nuclei with $A > 190$ (and many with $150 < A < 190$) are energetically unstable against α emission but only about one-half of them can meet these other requirements.

8.2 BASIC α DECAY PROCESSES

The spontaneous emission of an α particle can be represented by the following process:

$$ {}^{A}_{Z}X_{N} \rightarrow {}^{A-4}_{Z-2}X'_{N-2} + \alpha $$

The α particle, as was shown by Rutherford, is a nucleus of ^{4}He, consisting of two neutrons and two protons. To understand the decay process, we must study the conservation of energy, linear momentum, and angular momentum.

Let's first consider the conservation of energy in the α decay process. We assume the initial decaying nucleus X to be at rest. Then the energy of the initial system is just the rest energy of X, $m_X c^2$. The final state consists of X′ and α, each of which will be in motion (to conserve linear momentum). Thus the final total energy is $m_{X'}c^2 + T_{X'} + m_\alpha c^2 + T_\alpha$, where T represents the kinetic energy of the final particles. Thus conservation of energy gives

$$ m_X c^2 = m_{X'}c^2 + T_{X'} + m_\alpha c^2 + T_\alpha \qquad (8.1) $$

or

$$ (m_X - m_{X'} - m_\alpha)c^2 = T_{X'} + T_\alpha \qquad (8.2) $$

The quantity on the left side of Equation 8.2 is the net energy released in the decay, called the Q value:

$$Q = (m_X - m_{X'} - m_\alpha)c^2 \tag{8.3}$$

and the decay will occur spontaneously only if $Q > 0$. (The decay Q values for ^{232}U were listed in Table 8.1.) Q values can be calculated from *atomic* mass tables because even though Equation 8.3 represents a *nuclear* process, the electron masses will cancel in the subtraction. When the masses are in atomic mass units (u), expressing c^2 as 931.502 MeV/u gives Q values directly in MeV.

The Q value is also equal to the total kinetic energy given to the decay fragments:

$$Q = T_{X'} + T_\alpha \tag{8.4}$$

If the original nucleus X is at rest, then its linear momentum is zero, and conservation of linear momentum then requires that X′ and α move with equal and opposite momenta in order that the final momentum also be zero:

$$p_\alpha = p_{X'} \tag{8.5}$$

α decays typically release about 5 MeV of energy. Thus for both X′ and α, $T \ll mc^2$ and we may safely use nonrelativistic kinematics. Writing $T = p^2/2m$ and using Equations 8.4 and 8.5 gives the kinetic energy of the α particle in terms of the Q value:

$$T_\alpha = \frac{Q}{(1 + m_\alpha/m_{X'})} \tag{8.6}$$

Because the mass ratio is small compared with 1 (recall that X represents a heavy nucleus), it is usually sufficiently accurate to express this ratio simply as $4/(A - 4)$, which gives, with $A \gg 4$,

$$T_\alpha = Q(1 - 4/A) \tag{8.7}$$

Typically, the α particle carries about 98% of the Q value, with the much heavier nuclear fragment X′ carrying only about 2%. (This *recoil* energy of the heavy fragment is not entirely negligible. For a typical Q value of 5 MeV, the recoiling nucleus has an energy of the order of 100 keV. This energy is far in excess of that which binds atoms in solids, and thus the recoiling nucleus, if it is near the surface of the radioactive source, escapes from the source and can spread to the surroundings. If the α decay is part of a decay chain, then the recoiling daughter nucleus may itself be radioactive, and these recoils can result in the spread of radioactive material. Fortunately, the heavy recoil nuclei have an extremely short range in matter and their spread can be prevented by a thin coating, such as Mylar or lacquer, placed over the radioactive sample.)

The kinetic energy of an α particle can be measured directly with a magnetic spectrometer, and so the Q value of a decay can be determined. This gives us a way to determine atomic masses, such as in a case in which we might know the mass of long-lived X as a result of direct measurement but X′ is so short-lived that its mass cannot be determined by direct measurement.

8.3 α DECAY SYSTEMATICS

One feature of α decay is so striking that it was noticed as long ago as 1911, the year that Rutherford "discovered" the nucleus. Geiger and Nuttall noticed that α emitters with large disintegration energies had short half-lives and conversely. The variation is astonishingly rapid as we may see from the limiting cases of ^{232}Th (1.4×10^{10} y; $Q = 4.08$ MeV) and ^{218}Th (1.0×10^{-7} s; $Q = 9.85$ MeV). A factor of 2 in energy means a factor of 10^{24} in half-life! The theoretical explanation of this Geiger-Nuttall rule in 1928 was one of the first triumphs of quantum mechanics.

A plot of log $t_{1/2}$ against Q in which all α emitters are included shows a considerable scatter about the general Geiger-Nuttall trend. Very smooth curves result, however, if we plot only α emitters with the same Z and if further we select from this group only those with Z and N both even (Figure 8.1). Even-odd, odd-even, and odd-odd nuclei obey the general trend but do not plot into quite such smooth curves; their periods are 2–1000 times longer than those for even-even types with the same Z and Q.

It is interesting that ^{235}U (even Z, odd N) is one of these "extra-long-life" types. If its half-life were 1000 times shorter, this important nucleus would not occur in nature, and we probably would not have nuclear reactors today! We see in Chapter 13 that the same feature that apparently accounts for the long life against α decay, namely the odd neutron, also makes ^{235}U very susceptible to fission by thermal neutrons.

Figure 8.2 shows another important systematic relationship for α emitters. Looking for the moment only at the data for $A > 212$, we see that adding neutrons to a nucleus reduces the disintegration energy, which, because of the

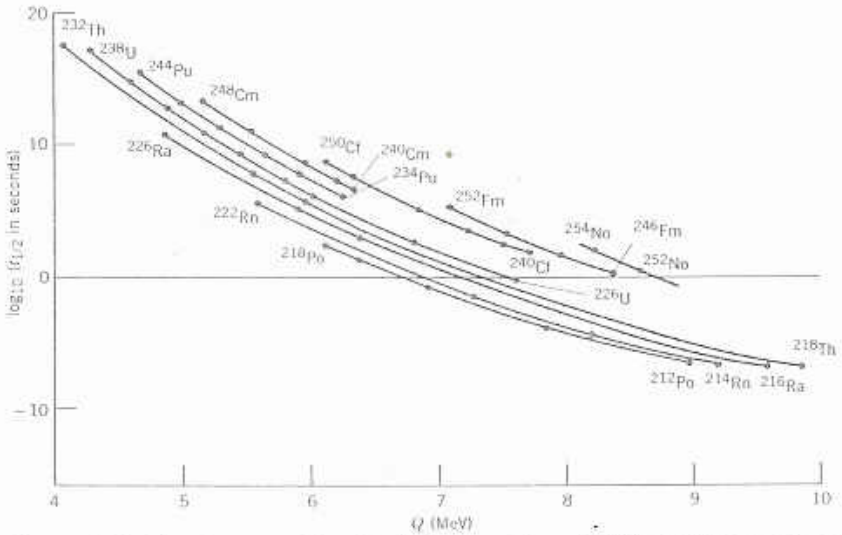

Figure 8.1 The inverse relationship between α-decay half-life and decay energy, called the Geiger-Nuttall rule. Only even-Z, even-N nuclei are shown. The solid lines connect the data points.

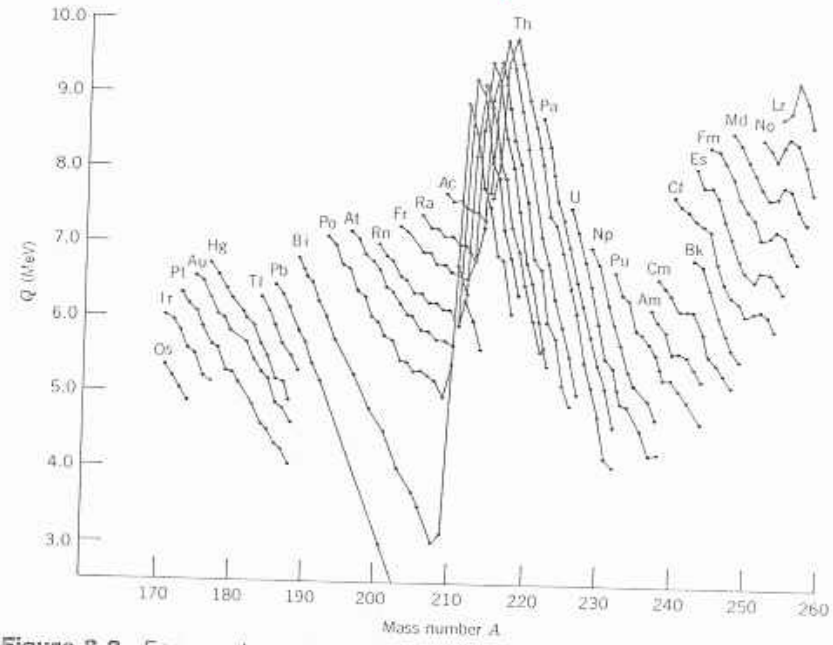

Figure 8.2 Energy released in α decay for various isotopic sequences of heavy nuclei. In contrast to Figure 8.1, both odd-A and even-A isotopes are shown, and a small amount of odd-even staggering can be seen. The effects of the shell closures at $N = 126$ (large dip in data) and $Z = 82$ (larger than average spacing between Po, Bi, and Pb sequences) are apparent.

Geiger-Nuttall rule, increases the half-life. The nucleus becomes more stable. A striking discontinuity near $A = 212$ occurs where $N = 126$ and is another example of nuclear shell structure.

We can compare the systematic dependence of Q on A with the prediction of the semiempirical mass formula, Equation 3.28.

$$Q = B(^4\text{He}) + B(Z-2, A-4) - B(Z, A) \tag{8.8}$$

$$\approx 28.3 - 4a_v + \tfrac{8}{3}a_s A^{-1/3} + 4a_c Z A^{-1/3}(1 - Z/3A)$$

$$-4a_{\text{sym}}(1 - 2Z/A)^2 + 3a_p A^{-7/4} \tag{8.9}$$

where the approximation in Equation 8.9 is $Z, A \gg 1$. For ^{226}Th, this formula gives $Q = 6.75$ MeV, not too far from the measured value of 6.45 MeV. What is perhaps more significant is that the general trend of Figure 8.2 is reproduced: for ^{232}Th, Equation 8.9 gives $Q = 5.71$ MeV (to be compared with $Q = 4.08$ MeV), while for ^{220}Th the formula gives $Q = 7.77$ MeV (compared with $Q = 8.95$ MeV). Keep in mind that the parameters of the semiempirical mass formula are chosen to give rough agreement with observed binding energies across the entire range of nuclei. It is important that the formula gives us rough agreement with the decay Q values and that it correctly gives $Q > 0$ for the heavy nuclei. It also

is more than the total available energy Q. Classically the α particle cannot enter this region from either direction, just as a tennis ball dropped from a certain height cannot rebound higher; in each case the kinetic energy would have to be negative. The region $r > b$ is a classically permitted region outside the barrier.

From the classical point of view, an α particle in the spherical potential well would sharply reverse its motion every time it tried to pass beyond $r = a$. Quantum mechanically, however, there is a chance of "leakage" or "tunnelling" through such a barrier. This barrier accounts for the fact that α-unstable nuclei do not decay immediately. The α particle within the nucleus must present itself again and again at the barrier surface until it finally penetrates. In ^{238}U, for example, the leakage probability is so small that the α particle, on the average, must make $\sim 10^{38}$ tries before it escapes ($\sim 10^{21}$ per second for $\sim 10^{9}$ years)!

The barrier also operates in reverse, in the case of α-particle scattering by nuclei (see Sections 3.1 and 11.6). Alpha particles incident on the barrier from outside the nucleus usually scatter in the Coulomb field if the incident energy is well below the barrier height. Tunnelling through the barrier, so that the nuclear force between the particle and target can cause nuclear reactions, is a relatively improbable process at low energy. The theoretical analysis of nuclear reactions induced by charged particles uses a formalism similar to that of α decay to calculate the barrier penetration probability. Fusion reactions, such as those responsible for the energy released in stars, also are analyzed using the barrier penetration approach (see Section 14.2).

The disintegration constant of an α emitter is given in the one-body theory by

$$\lambda = fP \tag{8.10}$$

where f is the frequency with which the α particle presents itself at the barrier and P is the probability of transmission through the barrier.

Equation 8.10 suggests that our treatment is going to be semiclassical in that our discussion of the situation for $r < a$ is very "billiard-ballish." A rigorous wave-mechanical treatment, however, gives about the same results for this problem. The quantity f is roughly of the order of v/a where v is the relative velocity of the α particle as it rattles about inside the nucleus. We can find v from the kinetic energy of the α particle for $r < a$. Estimating $V_0 \approx 35$ MeV for a typical well depth gives $f \approx 6 \times 10^{21}$/s for $Q = 5$ MeV. We will see later that we do not need to know f very precisely to check the theory.

The barrier penetration probability P must be obtained from a quantum mechanical calculation similar to the one-dimensional problem discussed in Section 2.3. Let's first use the result of that calculation, Equation 2.39, to estimate the probability P. Of course, the calculation that led to Equation 2.39 was based on a one-dimensional rectangular barrier, which is not directly applicable to the $1/r$ Coulomb potential, but we can at least find a rough order-of-magnitude estimate. The result, Equation 2.39, depends on the width of the barrier and on its height (called V_0 for the rectangular barrier) above the energy E of the particle. The Coulomb barrier of Figure 8.3 has height B at $r = a$, where

$$B = \frac{1}{4\pi\epsilon_0}\frac{zZ'e^2}{a} \tag{8.11}$$

In this expression the α particle has charge ze and the daughter nucleus, which

correctly predicts the decrease of Q with increasing A for a sequence of isotopes such as those of thorium, although it gives too small a change of Q with A (the formula gives $\Delta Q = -0.17$ MeV per unit change in A, while for Th the observed average change is $\Delta Q = -0.40$ MeV per unit change in A).

8.4 THEORY OF α EMISSION

The general features of Figure 8.1 can be accounted for by a quantum mechanical theory developed in 1928 almost simultaneously by Gamow and by Gurney and Condon. In this theory an α particle is assumed to move in a spherical region determined by the *daughter* nucleus. The central feature of this *one-body model* is that the α particle is preformed inside the parent nucleus. Actually there is not much reason to believe that α particles do exist separately within heavy nuclei; nevertheless, the theory works quite well, especially for even-even nuclei. This success of the theory does not prove that α particles are preformed, but merely that they behave as if they were.

Figure 8.3 shows a plot, suitable for purposes of the theory, of the potential energy between the α particle and the residual nucleus for various distances between their centers. The horizontal line Q is the disintegration energy. Note that the Coulomb potential is extended inward to a radius a and then arbitrarily cut off. The radius a can be taken as the sum of the radius of the residual nucleus and of the α particle. There are three regions of interest. In the spherical region $r < a$ we are "inside" the nucleus and speak of a potential well of depth $-V_0$, where V_0 is taken as a positive number. Classically the α particle can move in this region, with a kinetic energy $Q + V_0$ but it cannot escape from it. The annular-shell region $a < r < b$ forms a potential barrier because here the potential energy

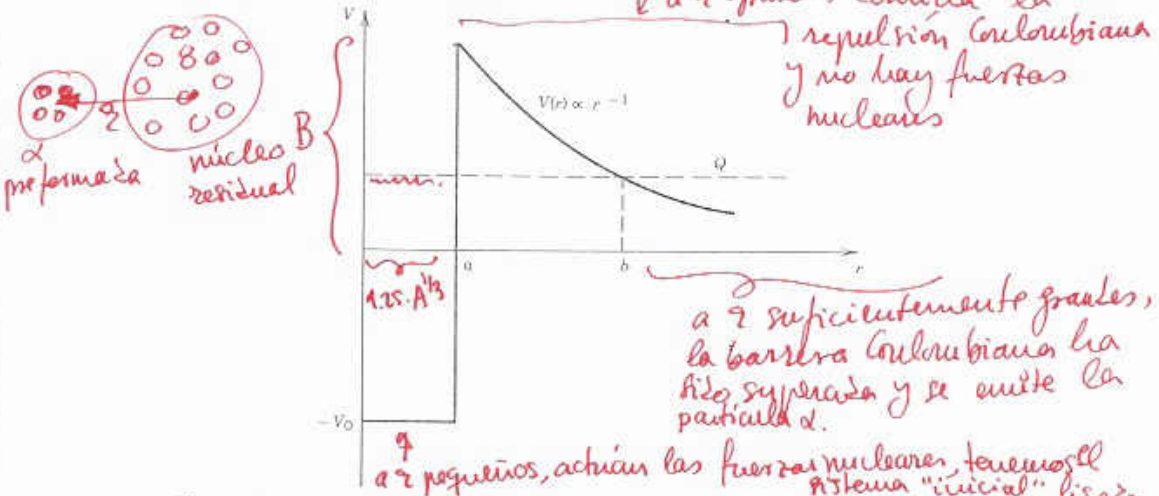

Figure 8.3 Relative potential energy of α-particle, daughter-nucleus system as a function of their separation. Inside the nuclear surface at $r = a$, the potential is represented as a square well; beyond the surface, only the Coulomb repulsion operates. The α particle tunnels through the Coulomb barrier from a to b.

provides the Coulomb repulsion, has charge $Z'e = (Z - z)e$. The height of the barrier thus varies from $(B - Q)$ above the particle's energy at $r = a$ to zero at $r = b$, and we can take a representative average height to be $\frac{1}{2}(B - Q)$. We can similarly choose a representative average width to be $\frac{1}{2}(b - a)$. The factor k_2 of Equation 2.39 then becomes $\sqrt{(2m/\hbar^2) \cdot \frac{1}{2}(B - Q)}$. For a typical heavy nucleus ($Z = 90$, $a = 7.5$ fm), the barrier height B is about 34 MeV, so the factor k_2 is about 1.6 fm^{-1}. The radius b at which the α particle "leaves" the barrier is found from the equality of the particle's energy and the potential energy:

$$b = \frac{1}{4\pi\epsilon_0}\frac{zZ'e^2}{Q} \tag{8.12}$$

and for a typical case of a heavy nucleus with $Q = 6$ MeV, $b = 42$ fm. Thus $k_2 \cdot \frac{1}{2}(b - a) \gg 1$ and we can approximate Equation 2.39 as

$$P \cong e^{-2k_2 \cdot (1/2)(b-a)} \tag{8.13}$$

since the factors in front of the exponential are of unit order of magnitude. For the case we are estimating here, $P \sim 2 \times 10^{-25}$ and thus $\lambda \sim 10^{-3}$/s and $t_{1/2} \sim 700$ s. A slight change of Q to 5 MeV changes P to 1×10^{-30} and $t_{1/2} \sim 10^8$ s. Even this very crude calculation is able to explain the many orders of magnitude change of $t_{1/2}$ between $Q = 5$ MeV and $Q = 6$ MeV, as illustrated in Figure 8.1.

The exact quantum mechanical calculation is very similar in spirit to the crude estimate above. We can think of the Coulomb barrier as made up of a sequence of infinitesimal rectangular barriers of height $V(r) = zZ'e^2/4\pi\epsilon_0 r$ and width dr. The probability to penetrate each infinitesimal barrier, which extends from r to $r + dr$, is

$$dP = \exp\left\{-2\,dr\sqrt{(2m/\hbar^2)[V(r) - Q]}\right\} \tag{8.14}$$

The probability to penetrate the complete barrier is

$$P = e^{-2G} \tag{8.15}$$

where the *Gamow factor* G is

$$G = \sqrt{\frac{2m}{\hbar^2}}\int_a^b [V(r) - Q]^{1/2}\,dr \tag{8.16}$$

which can be evaluated as

$$G = \sqrt{\frac{2m}{\hbar^2 Q}}\frac{zZ'e^2}{4\pi\epsilon_0}\left[\arccos\sqrt{x} - \sqrt{x(1-x)}\right] \tag{8.17}$$

where $x = a/b = Q/B$. The quantity in brackets in Equation 8.17 is approximately $\pi/2 - 2x^{1/2}$ when $x \ll 1$, as is the case for most decays of interest. Thus the result of the quantum mechanical calculation for the half-life of α decay is

$$t_{1/2} = 0.693\frac{a}{c}\sqrt{\frac{mc^2}{2(V_0 + Q)}}\exp\left\{2\sqrt{\frac{2mc^2}{(\hbar c)^2 Q}}\frac{zZ'e^2}{4\pi\epsilon_0}\left(\frac{\pi}{2} - 2\sqrt{\frac{Q}{B}}\right)\right\} \tag{8.18}$$

Table 8.2 Calculated α-Decay Half-lives for Th Isotopes

A	Q (MeV)	$t_{1/2}$ (s) Measured	$t_{1/2}$ (s) Calculated
220	8.95	10^{-5}	3.3×10^{-7}
222	8.13	2.8×10^{-3}	6.3×10^{-5}
224	7.31	1.04	3.3×10^{-2}
226	6.45	1854	6.0×10^{1}
228	5.52	6.0×10^{7}	2.4×10^{6}
230	4.77	2.5×10^{12}	1.0×10^{11}
232	4.08	4.4×10^{17}	2.6×10^{16}

The results of this calculation for the even isotopes of Th are shown in Table 8.2. The agreement is not exact, but the calculation is able to reproduce the trend of the half-lives within 1–2 orders of magnitude over a range of more than 20 orders of magnitude. We have neglected several important details in the calculation: we did not consider the initial and final nuclear wave functions (Fermi's Golden Rule, Equation 2.79, must be used to evaluate the decay probability), we did not consider the angular momentum carried by the α particle, and we assumed the nucleus to be spherical with a mean radius of $1.25A^{1/3}$ fm. The latter approximation has a very substantial influence on the calculated half-lives. The nuclei with $A \geq 230$ have strongly deformed shapes, and the calculated half-lives are extremely sensitive to small changes in the assumed mean radius. For instance, changing the mean radius to $1.20A^{1/3}$ (a 4% change in a) changes the half-lives by a factor of 5! In fact, because of this extreme sensitivity, the procedure is often reversed—the measured half-lives are used to deduce the nuclear radius; what actually comes out of the calculation is more like the sum of the radii of the nucleus X′ and the α particle, if we assume their charge distributions to have a sharp edge. This result can then be used to obtain an estimate of the nuclear radius; see, for example, L. Marquez, *J. Phys. Lett.* 42, 181 (1981).

Even though this oversimplified theory is not strictly correct, it gives us a good estimate of the decay half-lives. It also enables us to understand why other decays into light particles are not commonly seen, even though they may be allowed by the Q value. For example, the decay $^{220}\text{Th} \rightarrow {}^{12}\text{C} + {}^{208}\text{Po}$ would have a Q value of 32.1 MeV, and carrying through the calculation using Equation 8.18 gives $t_{1/2} = 2.3 \times 10^{6}$ s for the ^{220}Th decay into ^{12}C. This is a factor of 10^{13} longer than the α-decay half-life and thus the decay will not easily be observable.

Recently, just such a decay mode has in fact been observed, the first example of a spontaneous decay process involving emission of a particle heavier than an α. The decay of ^{223}Ra normally proceeds by α emission with a half-life of 11.2 d, but there has now been discovered the decay process $^{223}\text{Ra} \rightarrow {}^{14}\text{C} + {}^{209}\text{Pb}$. The probability for this process is very small, about 10^{-9} relative to the α decay. Figure 8.4 indicates the heroic efforts that are necessary to observe the process. To confirm that the emitted particle is ^{14}C requires the $\Delta E \cdot T$ technique discussed in Chapter 7. Figure 8.4 shows a portion of the high-energy end of the tail of the hyperbola expected for observation of carbon. From the mass tables,

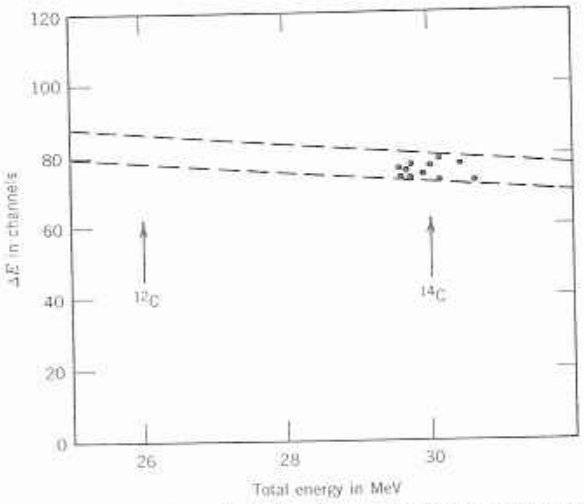

Figure 8.4 A portion of the tail of the $\Delta E \cdot T$ hyperbola showing the observed ^{14}C events from the decay of ^{223}Ra. The dashed lines show the limits expected for carbon. The 11 ^{14}C events result from 6 months of counting. From H. J. Rose and G. A. Jones, *Nature* **307**, 245 (1984). Reprinted by permission, copyright © Macmillan Journals Limited.

the decay Q value is calculated to be 31.8 MeV, which (when corrected for the recoil) gives a ^{14}C kinetic energy of 29.8 MeV. By contrast, the calculated energy for ^{12}C emission would be about 26 MeV. The total of 11 events observed represents about *six months* of counting with a source of 3.3 μCi of ^{223}Ra in secular equilibrium with 21-y ^{227}Ac, a member of the naturally occurring actinium series beginning with ^{235}U.

Calculating the Gamow factor for ^{14}C emission gives a decay probability of about 10^{-3} relative to α emission; the discrepancy between the calculated and observed (10^{-9}) values results from the assumptions about the preformation of the particle inside the nucleus. You will recall that our theory of α decay is based on the assumption that the α is preformed inside the nucleus. What the experiment tells us is that the probability for forming ^{14}C clusters inside the nucleus is about 10^{-6} relative to the probability to preform α's.

For a description of the experiment, see H. J. Rose and G. A. Jones, *Nature* **307**, 245 (1984). Emission of ^{14}C from several other nuclei in this region has also been observed, and emission of heavier decay fragments, including ^{24}Ne, has been reported.

Going in the opposite direction, we can use Equation 8.18 with $z = 1$ to evaluate the half-life for proton decay—that is, the spontaneous emission of a proton by an unstable nucleus. In this case the Coulomb barrier will be only half as high as it is for α decay, but these decays are inhibited for a stronger reason: the Q values for proton decay are generally negative and so the decays are absolutely forbidden by energy conservation. Such decays have recently been observed for a few proton-rich unstable nuclei, which are formed in nuclear reactions by bombarding a target with $N \approx Z$ using a projectile having $N \approx Z$.

tablas de masas y otras propiedades: http://nucleardata.nuclear.se/database/masses/

(95)

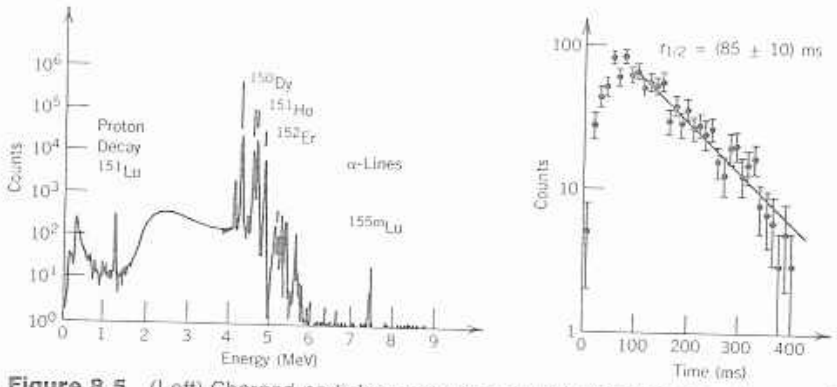

Figure 8.5 (Left) Charged-particle spectrum emitted in the radioactive decays of products of the reaction $^{96}Ru + ^{58}Ni$. The peaks above 4 MeV represent α decays; the 1.2-MeV peak is from proton emission. (Right) The decay with time of the proton peak gives a half-life of 85 ms. From S. Hofmann et al., *Z. Phys. A* **305**, 111 (1982).

This creates a heavy nucleus with $N \approx Z$, a very unstable configuration, and proton emission may be energetically possible, as the nucleus tries to relieve itself of its proton excess. The Q value for proton decay can be found by a slight modification of Equation 8.3, which gives exactly the negative of the proton separation energy, Equation 3.27. Proton decay will be energetically possible when the Q value is positive and therefore when the separation energy is negative. A glance at the mass tabulations (see A. H. Wapstra and G. Audi, *Nucl. Phys. A* **432**, 1 (1985)) shows only a few very rare cases in which the proton separation energy is negative, and even these are not directly measured but instead obtained by extrapolations from more stable nuclei.

In an experiment reported by Hofmann *et al.*, *Z. Phys. A* **305**, 111 (1982), a target of ^{96}Ru was bombarded with ^{58}Ni projectiles. Figure 8.5 shows the spectrum of light particles emitted following the reaction. The more energetic peaks are identified as α decays from unstable nuclei in the neighborhood of $A = 150$ produced in the reaction. The peak at 1.239 MeV was identified as a proton using ΔE-E techniques as described in Chapter 7. Its half-life was measured as 85 ms, as shown in Figure 8.5. The decay was assigned to the isotope ^{151}Lu based on a series of indirect arguments; unfortunately, reactions such as this produce many different products, and it is often a difficult task to identify the source of the observed radiations. This experiment thus provides evidence for the decay $^{151}Lu \rightarrow ^{150}Yb + p$.

Study of decays such as this enables us to extend our knowledge of nuclear mass systematics far beyond the previous limits; for instance, at the time of this work ^{151}Lu was three protons further from stability than the previous last known isobar (^{151}Er). Figure 8.6 shows the Q_p values deduced from known masses and from extrapolations based on systematics. The value for ^{151}Lu lies right on the theoretical calculation, giving confidence to both the identification of the isotope and to the theoretical calculation.

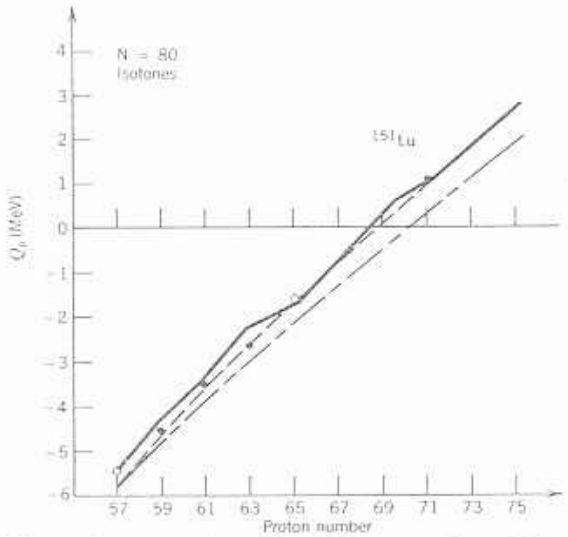

Figure 8.6 Proton-decay energies of $N = 80$ isotones. The solid lines are theoretical calculations based on nuclear mass formulas (somewhat like the semiempirical mass formula). Only for ^{151}Lu is the decay energy positive. From S. Hofmann et al., *Z. Phys. A* **305**, 111 (1982).

Using Equation 8.18 for the half-life gives a value of about 1.7 μs, too small by nearly 5 orders of magnitude. For this reason, it has been proposed that the decay is inhibited by differences in the nuclear structure of the initial and final states (or possibly by a large angular momentum change in the decay, examples of which are discussed in the next section).

8.5 ANGULAR MOMENTUM AND PARITY IN α DECAY

We have up to this point neglected to discuss the angular momentum carried by the α particle. In a transition from an initial nuclear state of angular momentum I_i to a final state I_f, the angular momentum of the α particle can range between $I_i + I_f$ and $|I_i - I_f|$. The nucleus ^{4}He consists of two protons and two neutrons, all in 1s states and all with their spins coupled pairwise to 0. The spin of the α particle is therefore zero, and the total angular momentum carried by an α particle in a decay process is purely orbital in character. We will designate this by ℓ_α. The α particle wave function is then represented by a $Y_{\ell m}$ with $\ell = \ell_\alpha$; thus the parity change associated with α emission is $(-1)^{\ell_\alpha}$, and we have a parity *selection rule*, indicating which transitions are permitted and which are absolutely forbidden by conservation of parity: if the initial and final parities are the same, then ℓ_α must be even; if the parities are different, then ℓ_α must be odd.

To study the applications of these rules, we must recognize that we have also neglected one very significant feature of α decay—a given initial state can populate many different final states in the daughter nucleus. This property is

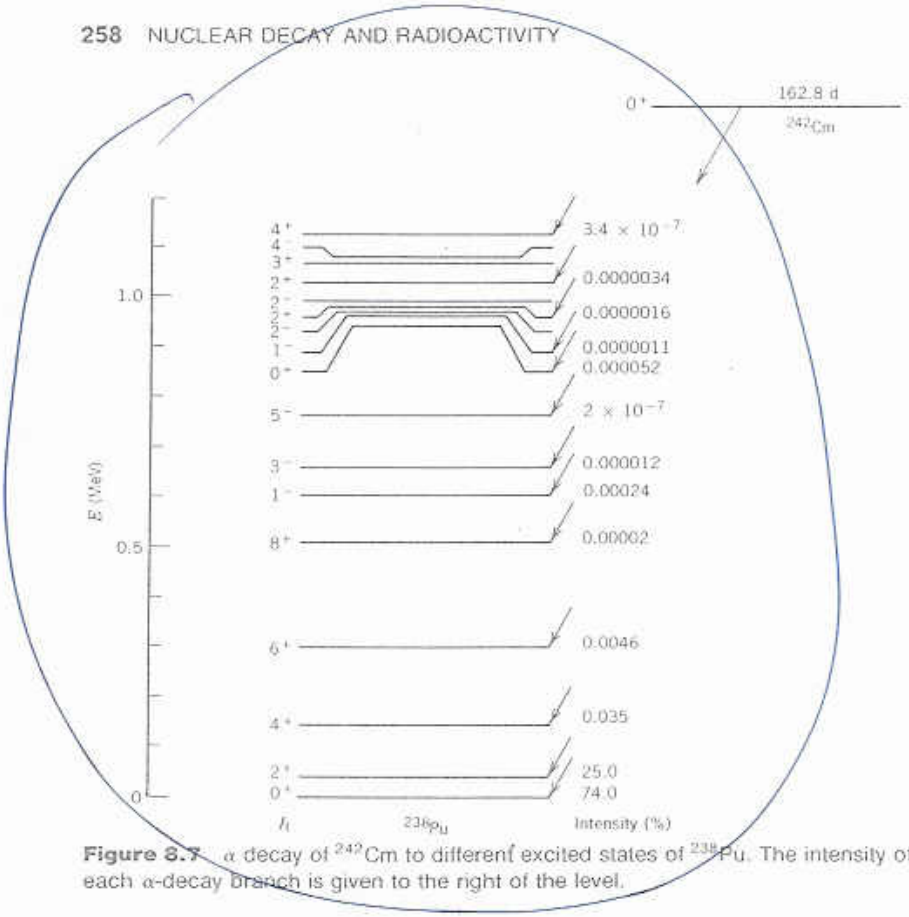

Figure 8.7 α decay of ^{242}Cm to different excited states of ^{238}Pu. The intensity of each α-decay branch is given to the right of the level.

sometimes known as the "fine structure" of α decay, but of course has nothing whatever to do with atomic fine structure. Figure 8.7 shows the α decay of ^{242}Cm. The initial state is spin zero, and thus the angular momentum of the α particle ℓ_α is equal to the angular momentum of the final nuclear state I_f. You can see that many different states of ^{238}Pu are populated. The α decays have different Q values (given by the Q value for decay to the ground state, 6.216 MeV, less the excitation energy of the excited state) and different intensities. The intensity depends on the wave functions of the initial and final states, and also depends on the angular momentum ℓ_α. In Equation 2.60, it was shown how the "centrifugal potential" $\ell(\ell+1)\hbar^2/2mr^2$ must be included in spherical coordinates. This term, which is always positive, has the effect of raising the potential energy for $a < r < b$ and thus increasing the thickness of the barrier which must be penetrated. Consider for example the 0^+, 2^+, 4^+, 6^+, and 8^+ states of the ground-state rotational band. The decay to the 2^+ state has less intensity than the decay to the ground state for two reasons—the "centrifugal potential" raises the barrier by about 0.5 MeV, and the excitation energy lowers Q by 0.044 MeV. The decay intensity continues to decrease for these same reasons as we go up the band to the 8^+ state. If we use our previous theory for the decay rates, taking

into account the increasing effective B and decreasing Q, we obtain the following estimates for the relative decay branches: 0^+, 76%; 2^+, 23%; 4^+, 1.5%; 6^+, 0.077%; 8^+, 8.4×10^{-5}%. These results are not in exact agreement with the observed decay intensities, but they do give us a rough idea of the origin of the decrease in intensity.

Once we go above the ground-state band, the α decay intensities become very small, of the order of 10^{-6}% of the total decay intensity. This situation results from the poor match of initial and final wave functions—many of these excited states originate with vibrations or pair-breaking particle excitations, which are not at all similar to the paired, vibrationless 0^+ ground state of ^{242}Cm. You should note that there are some states for which there is no observed decay intensity at all. These include the 2^- states at 0.968 and 0.986 MeV, the 3^+ state at 1.070 MeV, and the 4^- state at 1.083 MeV. Alpha decay to these states is absolutely forbidden by the parity selection rule. For example, a $0 \rightarrow 3$ decay must have $\ell_\alpha = 3$, which must give a change in parity between initial and final states. Thus $0^+ \rightarrow 3^-$ is possible, but not $0^+ \rightarrow 3^+$. Similarly, $0 \rightarrow 2$ and $0 \rightarrow 4$

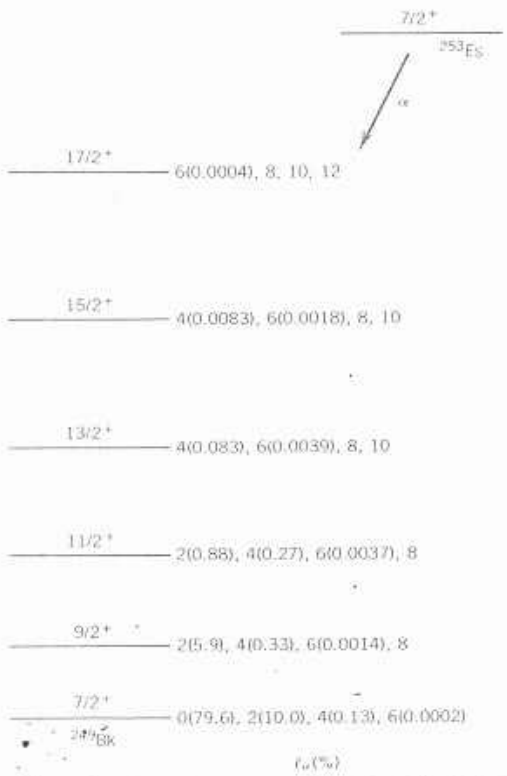

Figure 8.8 Intensities of various α-decay angular momentum components in the decay of ^{253}Es. For $\ell_\alpha = 8$ and higher, the intensities are not known but are presumably negligibly small. From the results of a study of spin-aligned α decays by A. J. Soinski et al., *Phys. Rev. C* **2**, 2379 (1970).

decays cannot change the parity, and so $0^+ \rightarrow 2^-$ and $0^+ \rightarrow 4^-$ are not permitted.

When neither the initial nor the final states have spin 0, the situation is not so simple and there are no absolutely forbidden decays. For example, the decay $2^- \rightarrow 2^+$ must have odd ℓ_α (because of the change in parity), and the angular momentum coupling rules require $0 \leq \ell_\alpha \leq 4$. Thus it is possible to have this decay with $\ell_\alpha = 1$ or 3. The next question that occurs is whether $\ell_\alpha = 1$ or $\ell_\alpha = 3$ is favored and by how much. Our previous discussion would lead us to guess that the $\ell_\alpha = 1$ intensity is roughly an order of magnitude greater than the $\ell_\alpha = 3$ intensity. However, measuring only the energy or the intensity of the decay gives us no information about how the total decay intensity is divided among the possible values of ℓ_α. To make the determination of the relative contributions of the different ℓ values, it is necessary to measure the angular distribution of the α particles. The emission of an $\ell = 1$ α particle is governed by a $Y_1(\theta, \phi)$, while an $\ell = 3$ α decay is emitted with a distribution according to $Y_3(\theta, \phi)$. If we determine the spatial distribution of these decays, we could in principle determine the relative amounts of the different ℓ values.

To do this experiment we must first align the spins of our α-radioactive nuclei, such as by aligning their magnetic dipole or electric quadrupole moments in a magnetic field or in a crystalline electric field gradient. Keeping the spins aligned requires that the nuclei must be cooled to a temperature at which the thermal motion is not sufficient to destroy the alignment; generally temperatures below 0.01 K are required (that is, less than 0.01 degree above the absolute zero of temperature!).

As an example of such an experiment, we consider the decay of ^{253}Es to states of the ground-state rotational band of ^{249}Bk. The possible ℓ values are indicated in Figure 8.8, and the results of measuring the α-particle angular distributions help us to determine the relative contribution of the different values of ℓ_α.

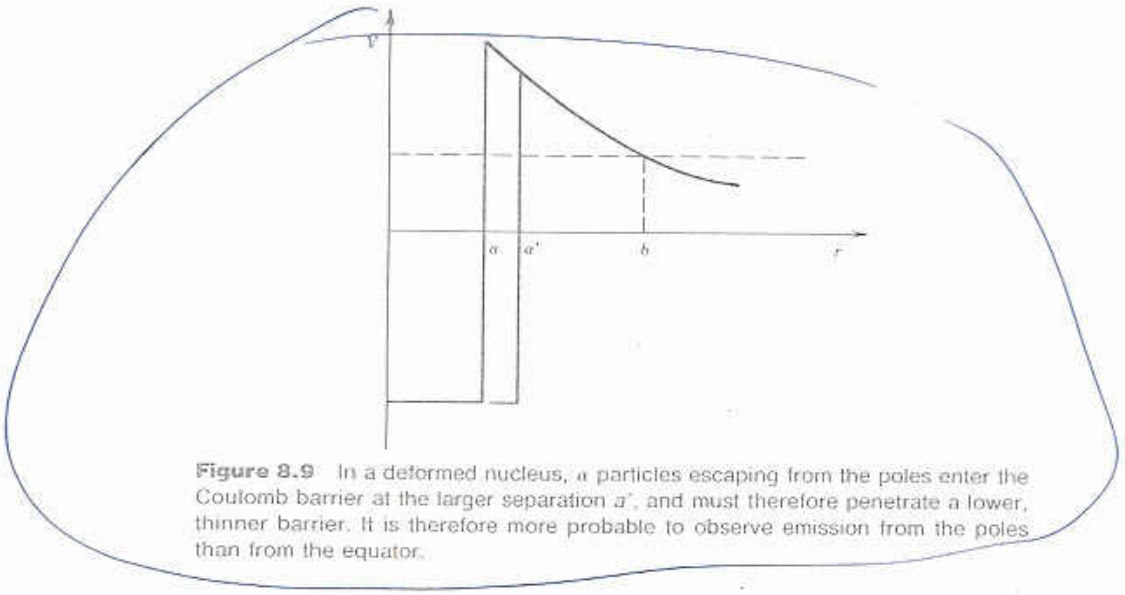

Figure 8.9 In a deformed nucleus, α particles escaping from the poles enter the Coulomb barrier at the larger separation a', and must therefore penetrate a lower, thinner barrier. It is therefore more probable to observe emission from the poles than from the equator.

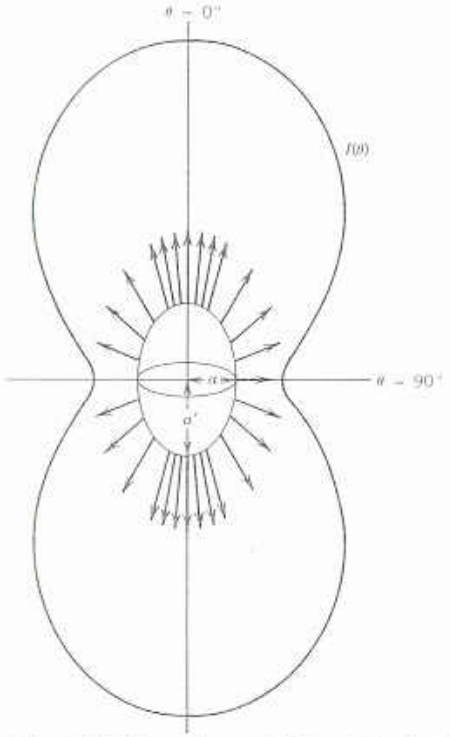

Figure 8.10 Intensity distribution of α particles emitted from the deformed nucleus at the center of the figure. The polar plot of intensity shows a pronounced angular distribution effect.

Since many α-emitting nuclei are deformed, these angular distribution measurements can also help us to answer another question: if we assume a stable prolate (elongated) nucleus, will more α's be emitted from the poles or from the equator? Figure 8.9 suggests a possible answer to this question: at the larger radius of the poles, the α particle feels a weaker Coulomb potential and must therefore penetrate a thinner and lower barrier. We therefore expect that polar emission ought to be more likely than equatorial emission. Figure 8.10 shows the angular distribution of α emission relative to the symmetry axis. You can see that emission from the poles is 3–4 times more probable than emission from the equator, exactly as we expect on the basis of the potential.

8.6 α DECAY SPECTROSCOPY

The final topic in our discussion of α decay is this: What can we learn about the energy levels of nuclei by studying α decay?

Let's consider, for example, the 5.3-h decay of ^{251}Fm to levels of ^{247}Cf. (The levels of ^{247}Cf are also populated in the beta decay of ^{247}Es, but the half-life of that decay is so short, 4.7 min, that it is more difficult to use as a detailed probe of the level structure of ^{247}Cf.)